Amyloid–Peptide Interactions

DOI: 10.1002/anie.201105877

Cross-Amyloid Interaction of Aβ and IAPP at Lipid Membranes**

*Janine Seeliger, Florian Evers, Christoph Jeworrek, Shobhna Kapoor, Katrin Weise, Erika Andreetto, Metin Tolan, Aphrodite Kapurniotu, and Roland Winter**

Several proteins and peptides are known to form cytotoxic oligomers and amyloid fibrils—mainly consisting of intermolecular cross-β-sheets—upon misfolding and self-association.[1] As these amyloid aggregates deposit in tissues, they are associated with cell degenerative diseases, such as type-2 diabetes mellitus (T2DM) or Alzheimer's disease (AD).[1] The present study is focused on the membrane-mediated aggregation of heteroassemblies of the islet amyloid polypeptide (IAPP) and the β-amyloid (Aβ) peptide. The extracellular deposits in the pancreas of patients with T2DM are mainly composed of the 37-residue IAPP, which is produced, stored, and secreted together with insulin by β-cells in the pancreatic islets of Langerhans.[2,3] The major component of the extracellular plaques in AD brains is Aβ, a 40- or 42-residue fragment of the membrane-associated amyloid precursor protein.[4,5] Recent clinical studies have pointed to a correlation between T2DM and AD, that is, patients with T2DM have a higher risk to suffer from AD and vice versa.[6] Remarkably, the sequences of IAPP and Aβ show a 25% identity and 50% similarity and it has been shown that fibrillation of IAPP can be cross-seeded by Aβ fibrils (Figure 1).[7] Most importantly, recent studies in vitro in the bulk phase have shown that early nonfibrillar and nontoxic Aβ and IAPP species bind each other with high affinity forming soluble, nonfibrillar, and nontoxic hetero-oligomers and that this interaction delays the cytotoxic self-association and amyloidogenesis of both Aβ and IAPP.[8] In this context, it has also been shown that the IAPP analogue [(N-Me)G24, (N-Me)I26]-IAPP or IAPP-GI, a mimic of non-amyloidogenic IAPP, forms nonfibrillar and nontoxic hetero-assemblies with Aβ and thus blocks the cytotoxic oligomer and fibril formation by Aβ.[8,12–14] As Aβ and IAPP are present in blood and cerebrospinal fluid at similar concentrations, an in vivo interaction might be possible, which could be a molecular link between AD and T2DM.[9–11]

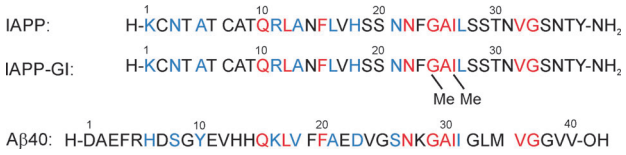

Figure 1. Primary structures of IAPP, the non-amyloidogenic IAPP mimic IAPP-GI, and Aβ40.[8,12] Identical residues between sequences are highlighted in red and similar residues are indicated in blue.[7]

Several studies have shown that lipid–peptide interactions can play a crucial role in amyloid formation of both IAPP and Aβ,[1,3,15–28] and the enhancement of fibrillation in the presence of membranes is believed to be causatively linked to the cellular damage caused by Aβ or IAPP assemblies.[25,26,28] Here, the interaction of IAPP and Aβ with a complex heterogeneous (raft-like) model biomembrane system comprising 15% DOPC, 10% DOPG, 40% DPPC, 10% DPPG, and 25% cholesterol has been studied. This lipid system allows for addressing effects of lateral heterogeneity (i.e., coexisting liquid-disordered and liquid-ordered domains) as well as charge effects upon peptide–membrane interactions. Both effects have been shown to be important for the membrane interaction of these peptides.[16,18,20,27,28] Furthermore, the cross-interaction of IAPP and Aβ in the presence of this membrane system was analyzed.

To gain a detailed picture of the membrane-mediated aggregation process of IAPP, Aβ, and their 1:1 mixture at the molecular level, both infrared spectroscopic and X-ray scattering techniques were applied. Monolayers of the lipid system were spread at the air–water interface and time-dependent changes in the vertical and lateral structure and in the packing properties of the membrane were analyzed by synchrotron X-ray reflectivity (XRR), grazing incidence X-ray diffraction (GIXD), and surface tensiometry. Time-dependent changes in the secondary structure of the peptides at a solid supported bilayer and the lipid–water interface were determined by attenuated total reflection Fourier-transform infrared (ATR-FTIR) spectroscopy and infrared reflection absorption spectroscopy (IRRAS), respectively. Finally, the interaction of Aβ with IAPP-GI under the experimental conditions described above was also studied (for details on the experimental procedures and techniques applied see Refs. [14,18,27,29] and the Supporting Information).

First, the lateral organization and structure of the bilayer and monolayer membrane systems were characterized. Similar to literature data, coexistence of liquid-ordered and

[*] J. Seeliger, C. Jeworrek, S. Kapoor, Dr. K. Weise, Prof. Dr. R. Winter
Physical Chemistry I—Biophysical Chemistry, Faculty of Chemistry, Technische Universität Dortmund
Otto-Hahn-Str. 6, 44227 Dortmund (Germany)
E-mail: roland.winter@tu-dortmund.de
Dr. F. Evers, Prof. Dr. M. Tolan
Faculty of Physics and DELTA, Technische Universität Dortmund
Maria-Goeppert-Mayer-Str. 2, 44221 Dortmund (Germany)
E. Andreetto, Prof. Dr. A. Kapurniotu
Division of Peptide Biochemistry, Technische Universität München
Emil-Erlenmeyer-Forum 5, 85354 Freising (Germany)

[**] Financial support from the DFG and the BMBF is gratefully acknowledged. We thank Oleg Konovalov and Alexei Vorobiev for their help setting up the X-ray scattering experiment and the ESRF for providing synchrotron radiation.

Supporting information for this article is available on the WWW under http://dx.doi.org/10.1002/anie.201105877.

liquid-disordered domains was found in giant unilamellar vesicles (GUVs) as well as in solid supported bilayers of the anionic lipid mixture.[29] By GIXD raft-like ordered domains were also detected in the corresponding monolayer system. The GIXD data reveal a single broad peak (Figure 2), indicating existence of hexagonally packed lipids in ordered crystalline-like domains. These small ordered domains are floating within a disordered, fluid-like lipid matrix (see the Supporting Information for details on the characterization of the lipid membranes).

The temporal changes of the secondary structure of 3 μM IAPP in the presence of the anionic raft bilayer were determined by ATR-FTIR spectroscopy (Figure 3a). The peak maximum of the amide-I′ band undergoes a strong shift from around 1645 cm^{-1} towards around 1621 cm^{-1}, indicating a decrease of disordered and α-helical structures and a concomitant increase of intermolecular β-sheets, pointing towards an aggregation of IAPP. As all normalized spectra seem to cross in an isosbestic kind of point (Figure 3a, right), the conversion of IAPP into the aggregated state appears to occur cooperatively from an essentially disordered confor-

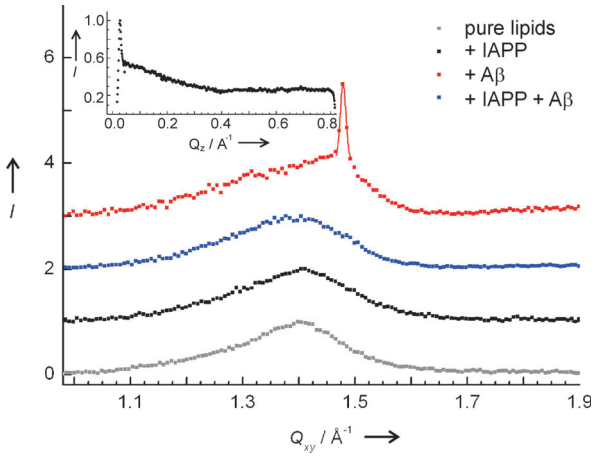

Figure 2. GIXD patterns $I(Q_{xy})$ of the anionic lipid raft monolayer on different peptide subphases. For clarity, data are shifted vertically. Inset: typical Bragg rod intensity profile $I(Q_z)$ obtained by integrating along the Q_{xy} region of the Bragg peak (here for the sample containing 250 nM Aβ); the absence of a peak at $Q_z \neq 0$ indicates little or no molecular tilt of the lipid tails.

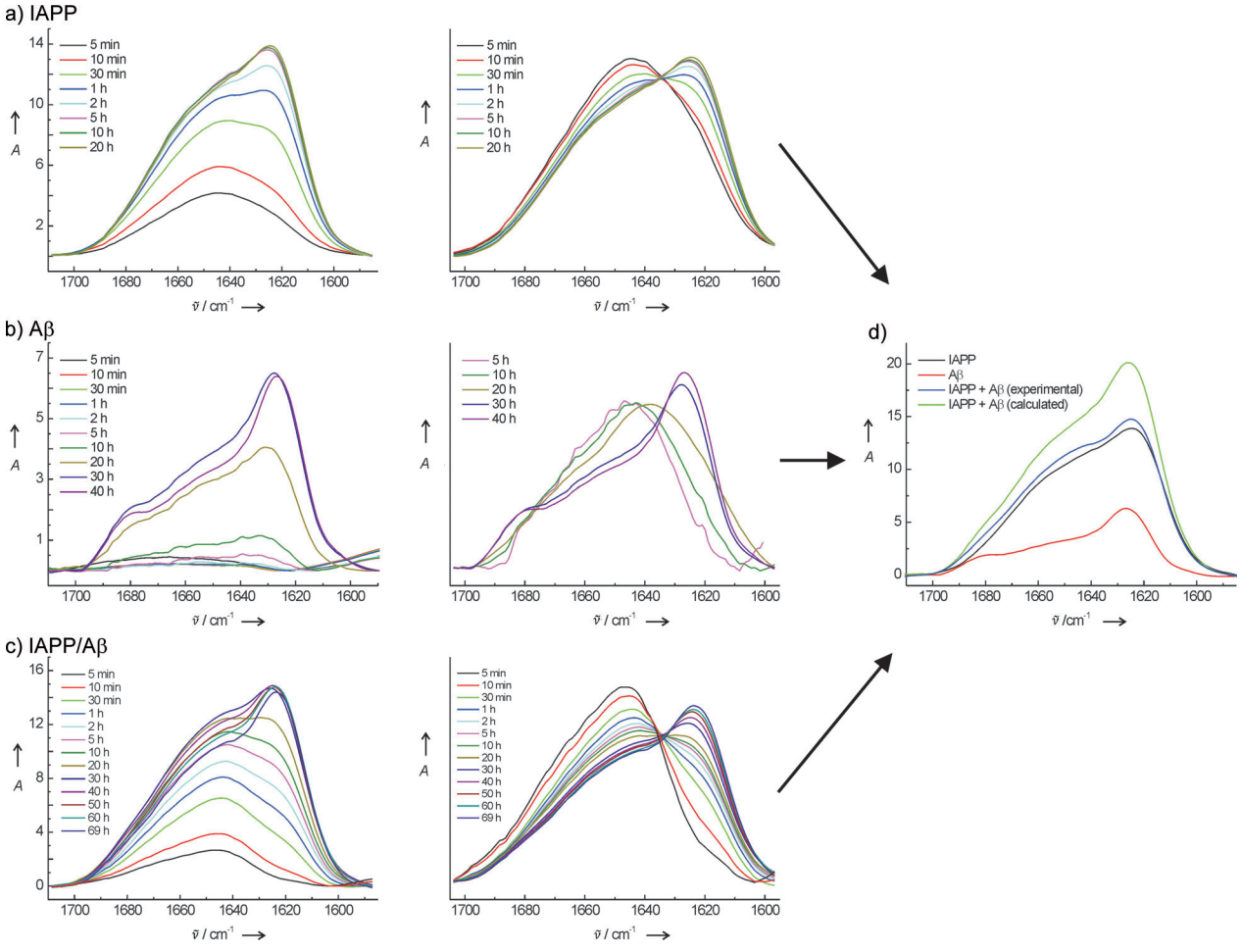

Figure 3. Shift of the amide-I′ band of a) IAPP (3 μM), b) Aβ (3 μM), and c) an equimolar IAPP–Aβ mixture (3 μM each) with time after injection into an ATR cell containing an anionic raft membrane at $T = 25\,°C$. Left: Primary ATR-FTIR spectra after buffer subtraction and baseline correction. Middle: Intensity normalization of the spectra shown on the left. d) Comparison of the ATR-FTIR spectra of IAPP (black) after 20 h, Aβ (red) after 40 h, and the IAPP–Aβ mixture (blue) after 40 h, that is, at time points where the aggregation/fibrillation process was completed, and a spectrum calculated from the sum of the pure IAPP and the pure Aβ spectra (green).

mation to the aggregated β-sheet containing form without largely populating intermediate structures containing other secondary structure motifs. IAPP aggregation and adsorption at the membrane occur essentially simultaneously. Hence, in accordance with literature data on homogeneous anionic lipid bilayers, IAPP penetrates readily into the lipid bilayer of this heterogeneous model biomembrane.[17,18] Together with these previous results and complementary AFM data (see Figure S10a in the Supporting Information), the results suggest that the IAPP assemblies (of ≈40% β-sheet content) that are present after 3 h of incubation in our experimental system are mature IAPP fibrils. Similar effects as observed by ATR-FTIR spectroscopy on the lipid bilayer membrane were also found by IRRAS measurements on the lipid raft monolayer, although the time scale of the process is different owing to the different experimental setups (see Figure S6 in the Supporting Information). In addition, the XRR results reveal that IAPP inserts into the head group region of the anionic lipid raft monolayer during the first 3 h (see Figure S5 in the Supporting Information). No significant changes of the GIXD patterns were recorded (Figure 2), suggesting that IAPP does not interact with the ordered raft-like domains, but rather partitions into the disordered domains of the heterogeneous lipid layer, which are rich in DOPG and DOPC.

GIXD measurements were performed at selected time points during the interaction of the lipid raft monolayer with a 250 nM Aβ solution (Figure 2). Remarkably, two signals were observed. The first, broad signal refers to the ordered domains and resembles that of the pure lipid layer. The second, sharp peak can be ascribed to additionally induced, but larger ordered domains, which most probably consist of ordered lipids (see the Supporting Information). Hence, the incorporation of Aβ would lead to a major reorganization of the lateral structure of the lipid monolayer. However, it cannot totally be ruled out that the sharp peak in the GIXD pattern is attributed to Aβ forming ordered β-sheet aggregates within the lipid monolayer. In the ATR-FTIR spectra of 3 μM Aβ at the anionic raft membrane (Figure 3b), the peak maximum of the amide-I′ band is shifting with time from an initial wavenumber of around 1655 cm^{-1}, which represents a mainly α-helical conformation, to around 1625 cm^{-1}, which is related to intermolecular β-sheet formation of an aggregated peptide (see Figure S8 in the Supporting Information for additional ATR-FTIR spectra at a higher concentration, 6 μM Aβ). In contrast to the IAPP aggregation process, Aβ aggregation does not occur by a direct spectroscopic conversion, but rather through the formation of intermediate states, indicated by a continuous spectral shift from α-helical/disordered conformations to β-sheet rich structures (≈40% after ≈40 h). These intermediate structures, probably on the oligomeric level, mainly consist of intra- and/or intermolecular β-sheets, both at a level of 20–25%. Similar results were obtained by the IRRAS monolayer measurements (see Figure S6 in the Supporting Information). In agreement with literature data, the aggregation of Aβ is a complicated multistep process consisting of several phases, which may incorporate lipid molecules as well.[22,25]

The effect of the interaction of IAPP with Aβ on their self-association in the presence of the anionic lipid raft bilayer membrane was studied by measuring an equimolar mixture of both peptides ($c = 3$ μM each) with ATR-FTIR spectroscopy (Figure 3c). In this case, the peak maximum of the amide-I′ band shifted from around 1645 cm^{-1} (mainly disordered structures) to around 1621 cm^{-1} (intermolecular β-sheets), similar to the behavior found for the pure IAPP. All normalized spectra seem to cross in an isosbestic kind of point, similar to pure IAPP (Figure 3a). This result and the fact that the spectra of IAPP and the mixture are nearly identical in shape and intensity after completion of the aggregation, but differ significantly from the pure Aβ as well as from the spectra calculated for the sum of pure IAPP and pure Aβ (Figure 3d), suggest that the assemblies present in the mixture show a structure resembling that of the assemblies present in the pure IAPP aggregates. This suggestion is further supported by the absence of a time-dependent β-sheet formation for an equimolar mixture of IAPP-GI and Aβ (see Figure S9 in the Supporting Information).[8] Here, mainly an adsorption at the lipid interface is observed and no indication for intermolecular β-sheet formation is obtained. These data are consistent with the previously reported inability of IAPP-GI to form β-sheet aggregates and with the findings that the IAPP-GI–Aβ heteroassemblies in bulk solution are non-fibrillar and noncytotoxic.[8,12,14]

The complementary IRRAS and XRR/GIXD measurements on the corresponding monolayer system corroborate these conclusions (see Figures S5/S6 in the Supporting Information): In the presence of both IAPP and Aβ, the IRRA profiles and electron density profiles indicate a combination of the processes observed for pure IAPP and Aβ. However, the GIXD experiments (Figure 2) reveal a similar lateral membrane organization upon addition of the peptide mixture as in the case of IAPP alone, and the Aβ-induced occurrence of a second ordered domain does not take place in the IAPP–Aβ–membrane mixture.

The comparison of the time dependence of intermolecular β-sheet formation of the incubations of Aβ or IAPP alone and the IAPP–Aβ mixture in the presence of the lipid membrane is presented in Figure 4. The ATR-FTIR data indicate formation of two stable structural assemblies in the IAPP–Aβ mixtures containing the same structure motifs, however in different amounts: the first one shows a content of around 29% β-sheets and forms within the first 3 h of incubation, which is nearly identical to the rate of IAPP self-association and markedly faster than the self-association of pure Aβ. Recently, detailed biophysical studies have shown that the interaction of Aβ and IAPP in the bulk initially results in formation of nonfibrillar and nontoxic heterooligomers.[8] Such heterooligomers are likely present between the time points of 7 and 15 h in the current experimental setup and convert thereafter in a very slow process to a second assembly that shows a β-sheet content of around 43%. Interestingly, a two-step self-assembly process was also observed for the Aβ alone incubation (see above). Notably, the β-sheet content of the IAPP–Aβ mixture at the end of the incubation process is identical to the contents of the Aβ alone or IAPP alone incubation. These results suggest that formation of a IAPP–Aβ heteroassembly with a β-sheet content of around 29% between 7 and 15 h under cellular membrane-like conditions

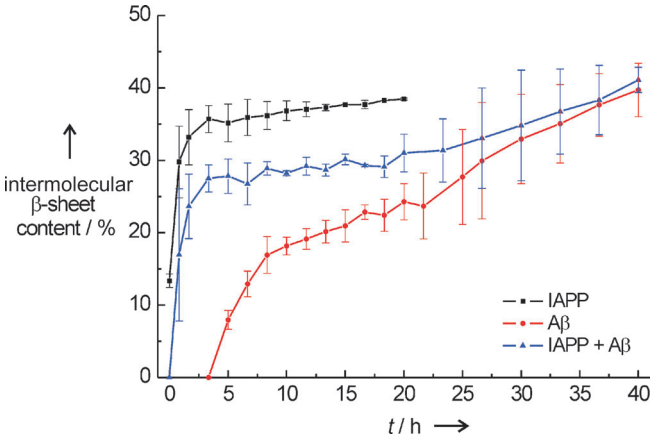

Figure 4. Time evolution of the intermolecular β-sheet content upon aggregation of 3 μM IAPP (black), 3 μM Aβ (red) and an equimolar IAPP–Aβ mixture (3 μM each, blue) at $T = 25\,^{\circ}C$ in the presence of an anionic lipid raft bilayer, derived from peak fitting of the normalized ATR-FTIR spectra.

delays but does not block fibrillation of IAPP and Aβ, and is thus in good agreement with the previously reported findings in the bulk.[8] By comparison, within this time frame solutions of IAPP alone consist mainly of "matured" IAPP aggregates, likely fibrils (as suggested by AFM), whereas in the respective Aβ alone solution, a fast transition of aggregates with 20% β-sheet structure toward aggregates with 43% β-sheets, likely fibrils, is observed.

Complementary AFM studies in the presence of an anionic mica interface, which may mimic the anionic lipid surface, support these data (see Figure S10 in the Supporting Information). They reveal only oligomeric species after 1 h of aggregation for the IAPP–Aβ mixture, whereas a large amount of fibrils is already visible for IAPP at this time point. For the equimolar mixture of IAPP and Aβ—next to oligomeric structures—protofibrils and short fibrils appear after about 4 h of aggregation.

In summary, the results of this study provide mechanistic insights into both the reported noncytotoxic nonfibrillar heteroassemblies between Aβ and the nonamyloidogenic IAPP-GI, as well as for the kinetic evolution of cell-toxic assemblies in mixtures of Aβ with the highly amyloidogenic IAPP under cellular membrane-like conditions. The mixture of both peptides is found to aggregate into β-sheets and fibrils slower as compared to pure IAPP. This behavior is similar to the one observed in the bulk.[8] The membrane-associated aggregate structures formed in the IAPP–Aβ heteroassembly have a structure that appears to be 1) very similar to the structure of the pure IAPP aggregates and 2) rather different from the structure of the Aβ aggregates (Figure 5). A complete cross-inhibition of the fibrillation process in the presence of the lipid membrane is not observed.

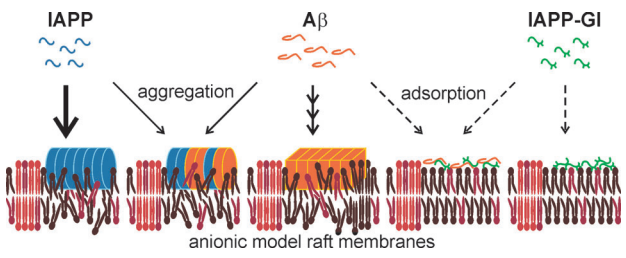

Figure 5. Interaction of IAPP, Aβ and equimolar IAPP–Aβ or IAPP-GI–Aβ mixtures in the presence of an anionic lipid raft bilayer membrane.

Received: August 19, 2011
Revised: October 19, 2011
Published online: December 1, 2011

Keywords: β-amyloids · fibril formation · IR spectroscopy · islet amyloid polypeptides · X-ray diffraction

[1] *Lipids and Cellular Membranes in Amyloid Diseases* (Ed.: R. Jelinek), Wiley-VCH, Weinheim, **2011**.
[2] G. J. Cooper, A. C. Willis, A. Clark, R. C. Turner, R. B. Sim, K. B. Reid, *Proc. Natl. Acad. Sci. USA* **1987**, *84*, 8628–8632.
[3] M. F. M. Engel, *Chem. Phys. Lipids* **2009**, *160*, 1–10.
[4] E. G. Zinser, T. Hartmann, M. O. W. Grimm, *Biochim. Biophys. Acta Biomembr.* **2007**, *1768*, 1991–2001.
[5] I. Morgado, M. Fändrich, *Curr. Opin. Colloid Interface Sci.* **2011**, *16*, 508–514.
[6] M. R. Nicolls, *Curr. Alzheimer Res.* **2004**, *1*, 47–54.
[7] B. O'Nuallain, A. D. Williams, P. Westermark, R. Wetzel, *J. Biol. Chem.* **2004**, *279*, 17490–17499.
[8] L. M. Yan, A. Velkova, M. Tatarek-Nossol, E. Andreetto, A. Kapurniotu, *Angew. Chem.* **2007**, *119*, 1268–1274; *Angew. Chem. Int. Ed.* **2007**, *46*, 1246–1252.
[9] T. Sanke, T. Hanabusa, Y. Nakano, C. Oki, K. Okai, S. Nishimura, M. Kondo, K. Nanjo, *Diabetologia* **1991**, *34*, 129–132.
[10] W. A. Banks, A. J. Kastin, L. M. Maness, W. Huang, J. B. Jaspan, *Life Sci.* **1995**, *57*, 1993–2001.
[11] N. Ida, T. Hartmann, J. Pantel, J. Schröder, R. Zerfass, H. Förstl, R. Sandbrink, C. L. Masters, K. Beyreuther, *J. Biol. Chem.* **1996**, *271*, 22908–22914.
[12] L. M. Yan, M. Tatarek-Nossol, A. Velkova, A. Kazantzis, A. Kapurniotu, *Proc. Natl. Acad. Sci. USA* **2006**, *103*, 2046–2051.
[13] E. Andreetto, L. M. Yan, M. Tatarek-Nossol, A. Velkova, R. Frank, A. Kapurniotu, *Angew. Chem.* **2010**, *122*, 3146–3151; *Angew. Chem. Int. Ed.* **2010**, *49*, 3081–3085.
[14] D. Sellin, L. M. Yan, A. Kapurniotu, R. Winter, *Biophys. Chem.* **2010**, *150*, 73–79.
[15] S. A. Jayasinghe, R. Langen, *Biochemistry* **2005**, *44*, 12113–12119.
[16] M. F. M. Engel, H. Yigittop, R. C. Elgersma, D. T. S. Rijkers, R. M. J. Liskamp, B. de Kruijff, J. W. M. Höppener, J. A. Killian, *J. Mol. Biol.* **2006**, *356*, 783–789.
[17] S. Jha, D. Sellin, R. Seidel, R. Winter, *J. Mol. Biol.* **2009**, *389*, 907–920.
[18] F. Evers, C. Jeworrek, S. Tiemeyer, K. Weise, D. Sellin, M. Paulus, B. Struth, M. Tolan, R. Winter, *J. Am. Chem. Soc.* **2009**, *131*, 9516–9521.
[19] C. Aisenbrey, T. Borowik, R. Byström, M. Bokvist, F. Lindström, H. Misiak, M. A. Sani, G. Gröbner, *Eur. Biophys. J.* **2008**, *37*, 247–255.
[20] K. Dahse, M. Garvey, M. Kovermann, A. Vogel, J. Balbach, M. Fändrich, A. Fahr, *J. Mol. Biol.* **2010**, *403*, 643–659.
[21] M. Bokvist, G. Gröbner, *J. Am. Chem. Soc.* **2007**, *129*, 14848–14849.
[22] G. P. Gellermann, T. R. Appel, A. Tannert, A. Radestock, P. Hortschansky, V. Schroeckh, C. Leisner, T. Lütkepohl, S. Shtrasburg, C. Röcken, M. Pras, R. P. Linke, S. Diekmann, M. Fändrich, *Proc. Natl. Acad. Sci. USA* **2005**, *102*, 6297–9302.

[23] C. Ege, J. Majewski, G. Wu, K. Kjaer, K. Y. C. Lee, *ChemPhysChem* **2005**, *6*, 226 – 229.
[24] E. Maltseva, A. Kerth, A. Blume, H. Möhwald, G. Brezesinski, *ChemBioChem* **2005**, *6*, 1817 – 1824.
[25] S. Askarova, X. Yang, J. C. M. Lee, *Int. J. Alzheimer's Disease* **2011**, Article ID 134971.
[26] S. M. Butterfield, H. A. Lashuel, *Angew. Chem.* **2010**, *122*, 5760 – 5788; *Angew. Chem. Int. Ed.* **2010**, *49*, 5628 – 5654.
[27] K. Weise, D. Radovan, A. Gohlke, N. Opitz, R. Winter, *ChemBioChem* **2010**, *11*, 1280 – 1290.
[28] D. H. J. Lopes, A. Meister, A. Gohlke, A. Hauser, A. Blume, R. Winter, *Biophys. J.* **2007**, *93*, 3132 – 3141.
[29] S. Kapoor, A. Werkmüller, C. Denter, Y. Zhai, J. Markgraf, K. Weise, N. Opitz, R. Winter, *Biochim. Biophys. Acta Biomembr.* **2011**, *1808*, 1187 – 1195.

